Anal. Bioanal. Electrochem., Vol. 11, No. 1, 2019, 19-37

Analytical & Bioanalytical Electrochemistry

2019 by CEE
www.abechem.com

Full Paper

A New Family of Borated Glasses as a Corrosion Inhibitor for Carbon Steel in Acidic Medium (1.0 M HCl)

Azeddine Elbadaoui,[1] Mouhsine Galai,[2,*] Soumya Ferraa,[1] Hanane Barebita,[1] Mohammed Cherkaoui[1] and Taoufiq Guedira[1]

[1]*Laboratory of Materials, Electrochemistry and Environment, Faculty of Science, Ibn Tofail University, Kénitra, Morocco*

[2]*Laboratory of Materials Engineering and Environment: Modelling and Application, University Ibn Tofail, Faculty of Sciences, Department of Chemistry, PO Box 133 – 14000- 16 Kenitra, Morocco*

*Corresponding Author, Tel.:(+212)677235695

E-Mail:galaimouhsine@gmail.com

Received: 7 August 2018 / Received in revised form: 16 December 2018 / Accepted: 21 December2018 / Published online: 31 January 2019

Abstract- The corrosion inhibition of carbon steel in acidic medium (1 M HCl) containing a borated vitreous glasses was studied by electrochemical technique (potentiodynamic polarization and electrochemical impedance spectroscopy).The various vitreous samples were synthesized from ammonium dihydrogen phosphate (NH_4) $2HPO_4$), the niobium oxide Nb_2O_5, the Bi_2O_3 bismuth oxide, the B_2O_3 boron oxide and the niobium oxide Nb_2O_5. The vitreous compositions are correlated with the system Bi_2O_3-B_2O_3- ($0.5Nb_2O_5$ -$0.5P_2O_5$) by stoichiometric mixing. These phases were characterized by X-ray diffraction (XRD) and infrared spectroscopy (IR). Polarization curve technique reveals that the inhibition efficiency E% increased with the concentration of the different borated vitreous which appears to be a anodic type inhibitors in the acidic medium. Electrochemical impedance spectroscopy confirms this result, indeed the transfer resistance increases with these compounds concentration. The action mechanism of vitreous phases has been elucidated by a thermodynamic study.

Keywords- Borated glasses, Corrosion inhibitor, Steel, 1.0 M Hydrochloric acid

1. INTRODUCTION

In many industrial, steel and its alloys are widely exposed to different aggressive environments. These environments inevitably lead to their attack. Among the protection methods of the most effective and least expensive may be mentioned the use of corrosion inhibitors [1-5]. The organic inhibitors are constituted by at least one heteroatom (nitrogen, oxygen or sulfur) active center of the molecule and have a high electron density. They would be adsorbed on the surface and form a protective film [6-8]. Inorganic compounds (chromates, phosphates, molybdates ...) stabilize the oxide layer on the metal surface or render more alkaline the corrosive medium [9-16]. In this work, our investigations were carried on the synthesis of inorganic compounds such as glasses borates and their application in corrosion. The prepared glasses were characterized by X-ray diffraction and infrared spectroscopy. The corrosion inhibition study was evaluated by polarization and electrochemical impedance.

In this work the novelty related to syntheses of two new borated vitreous glasses compounds to obtain a new variety of multifunctional glasses, for use as corrosion inhibitors of carbon steel in 1M HCl. The corrosion inhibition of these compounds was examined by electrochemical methods

2. EXPERIMENTAL DETAILS

2.1. Synthesis and preparation of borated vitreous glasses

The various vitreous samples were synthesized from ammonium dihydrogen phosphate $(NH_4)\ 2HPO_4$ (Reidel-Pool), the niobium oxide Nb_2O_5 (Aldrich), the Bi_2O_3 bismuth oxide (Aldrich), the B_2O_3 boron oxide (Aldrich) and the niobium oxide Nb_2O_5 (Fluka). The vitreous compositions are correlated with the system **Bi_2O_3-B_2O_3- ($0.5Nb_2O_5$ -$0.5P_2O_5$)** by stoichiometric mixing of raw materials according to the reaction scheme:

$(1\text{-}x\text{-}y)Bi_2O_3+xB_2O_3+y/2Nb_2O_5+y(NH_4)_2HPO\rightarrow$

$(1\text{-}x\text{-}y)\ Bi_2O_3 + xB_2O_3 + y/2Nb_2O_5 + y/2P_2O_5 + 2yNH_3+3y/2H_2O.$

The mixtures were crushed in an agate mortar. The thermal operation is conducted in alumina crucibles. The first treatment at 350 °C for 15 h allows the decomposition of hydrogen; it is followed by a homogenizing grinding. Each reaction mixture is then heated to 1050 °C, higher than the melting temperature and then dipped energetically in an aluminum mold preheated to 200 °C. The infra-red spectra are recorded entre 4000 and 400 cm^{-1} using a spectrometer with transformed Fourier of the kind Perkin Elmer1600. For XRD study, we used a Panalatycal Model X 'PERT powder 3, the radiation is $\lambda_{K\alpha}$(Cu)=1.5406 Å.

2.2. Electrochemical cell

The experiments were performed with carbon steel with surface area of 1 cm^2 as working electrode (weight in %, C=0,21, Mn=0,05, Si=0,38, S=0,05, P=0,09, Al=0,01), platinum counter electrode (CE) and a saturated calomel electrode (SCE) was used as a reference electrode . The work electrode was abraded with emery paper (up to 1200 grit), cleaned in acetone and washed by distillated water and finally dried at hot air before any electrochemical measurement. The concentrations of inhibitors were ranged from 100 to 300 ppm. The aggressive medium was HCl 1 mol / L.

2.2.1. Potentiodynamic polarization measurement

The Tafel polarization curves were recorded by scanning the electrode potential from - 900 mV/ECS to -100mV/ECS with a scanning rate of 1 mV/s. the calculate of corrosion kinetic parameters, by Stern-Geary equation fitting was used. For that, the potential domain not far from the corrosion potential ($^{+}$- 100 mV/SCE), it may be considered that both processes followed the Tafel law [24]. It can be extract from the following equation (1):

$$i = i_a + i_c = i_{corr}\left\{\exp\left[b_a \times \left(E - E_{corr}\right)\right] - \exp\left[b_c \times \left(E - E_{corr}\right)\right]\right\} \quad (1)$$

where:

-i_{corr} is the corrosion current density (A cm^{-2}),

- bc and ba are the Tafel constants of cathodic and anodic reactions (V^{-1}), respectively. The Tafel slopes *β(V/dec)* in usual logarithmic scale are given by following equation (2):

$$\beta = \frac{\ln 10}{b} = \frac{2.303}{b} \quad (2)$$

The electrochemical parameters were calculated by nonlinear regression method by applying equation (1) using Origin software 6.0 types.

For calculation of inhibition efficiency from the corrosion current densities we are using the relation (3):

$$\eta_{PP} = \frac{i^0_{corr} - i_{corr}}{i^0_{corr}} \times 100 \quad (3)$$

From the polarization curves for various concentrations of inhibitor we can extract the surface coverage (θ) by using the following equation [25]:

$$\theta = 1 - \frac{i_{corr}}{i^0_{corr}} \quad (4)$$

where i^{0}_{corr} and i_{corr} are the current densities of corrosion test in the absence and the presence without of inhibitor, respectively.

2.2.2. Electrochemical impedance spectroscopy measurements (EIS)

The electrochemical impedance spectroscopy measurements were carried out using a transfer function analyzer (VoltaLab PGZ 100), with a small amplitude a.c. signal (10 mV rms), over a frequency domain from 100 kHz to 100 mHz with five points per decade. The EIS diagrams were done in the Nyquist representation. The results were analyzed and fitted in terms of an equivalent electrical circuit using the simulation ZView 2.80

The inhibiting efficiency derived from EIS, η_{EIS} is also added and calculated using the following equation (5):

$$\eta_{EIS} = [(R_{ct} - R^{0}_{ct}) / R_{ct}]*100 \quad (5)$$

where R^{0}_{ct} and R_{ct} are the charge transfer resistance values in the absence and in the presence of inhibitor, respectively.

3. RESULTS AND DISCUSSION

3.1. Delimitation vitreous domain

The X-ray diffraction enabled to identify the vitreous compositions in the studied system. Any sample whose spectrum did not contain diffraction lines is considered as belonging to the vitreous system. Figure 1 shows the defined area. This system has already been subject to investigation [17-19].

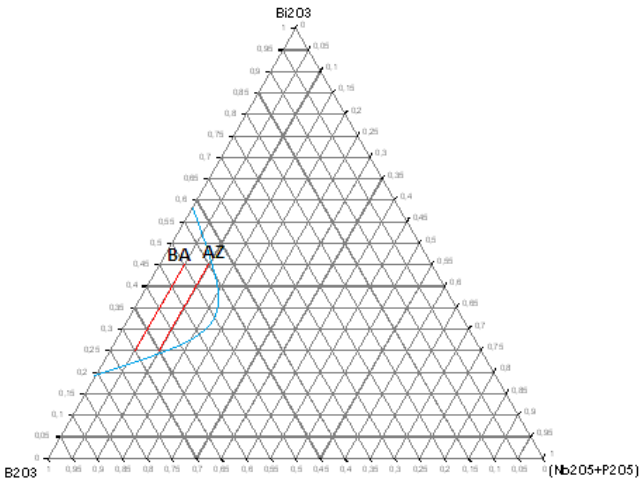

Fig. 1. Delimitation of Bi_2O_3-B_2O_3-[$0.5P_2O_5$-$0.5Nb_2O_5$] vitreous domain

Two axes of glassy system were studied:

- Axe **(**BA**)** :**(0.95-x) Bi_2O_3-x B_2O_3-0.05 [P_2O_5-Nb_2O_5]** with $0.3 \leq x \leq 0.5$
- Axe **(**AZ**)** : **(0.90-x) Bi_2O_3-x B_2O_3-0.1 [P_2O_5-Nb_2O_5]** with $0.3 \leq x \leq 0.5$.

Tables 1 and 2 give the corresponding molar fractions. Figure 2 shows the X-ray spectra for the AZ axis compositions. The diffraction spectrum of X-ray from the axis BA is substantially similar.

Table 1. Molar fractions of (0.95-x) Bi_2O_3-xB_2O_3- (0.025P_2O_5-0.025Nb_2O_5)

Sample	x	0.95-x
BA6	0.30	0.65
BA7	0.35	0.60
BA8	0.40	0.55
BA9	0.45	0.50
BA10	0.50	0.45

Table 2. Molar fractions of (0.90- x) Bi_2O_3-xB_2O_3-(0.05P_2O_5-0.05Nb_2O_5)

Sample	**x**	**0.90-x**
AZ6	0.3	0.6
AZ7	0.35	0.55
AZ8	0.4	0.5
AZ9	0.45	0.45
AZ10	0.5	0.4

3.2. X-ray diffraction

In addition, the X-ray diffraction (XRD) patterns of several compositions of the prepared of AZ axis samples are shown in Fig. 2. It is observed that homogenous glasses are formed for different concentration of B_2O_3.

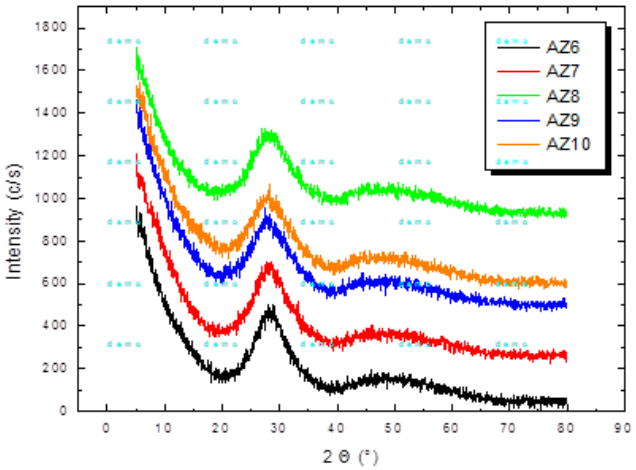

Fig. 2. XRD Spectrums of (0.90-x) Bi_2O_3-x B_2O_3-0.1 [P_2O_5-Nb_2O_5]

3.3. IR study

Figures 3 and 4 show the infrared spectra of (BA) and (AZ) axis respectively. The frequencies and powers are summarized in Tables 3 and 4.

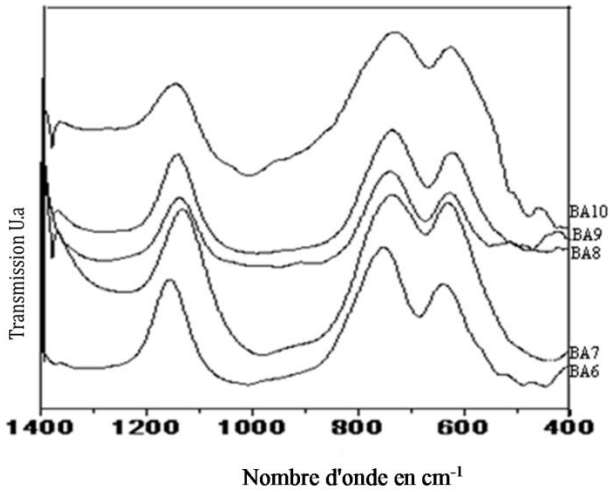

Fig. 3. IR Spectrums of (0.90-x) Bi_2O_3-x B_2O_3-0.05 [P_2O_5-Nb_2O_5]

We notice a widening of the bands. Indeed, in the glassy state, the molecules or groups of atoms are not isolated. These entities are in strong interaction with each other. In a glass sample, a unit cell can be defined and the entire sample must be considered as a single cell containing a giant molecule with an infinite number of entities that vibrate.

From figure 3, we noticed that the band between 420 cm^{-1} and 490 cm^{-1} is covering of various structural units. It can be attributed to the B-O-B vibrations [20-22]. The boron atoms in coordination IV are responsible for the appearance of the band between 500 cm^{-1}-540 cm^{-1} and the band at 750 cm^{-1} [23-24].The band between 600 cm^{-1}- 690 cm^{-1} was assigned to the

vibrations of the B-O-P bond in alkaline borophosphate glasses [20-29]. Scagliotti and Al have evoked bands around 1000 cm^{-1} related to O-P-O vibrations which do not appear in our spectrum [30]. The band between 1190 cm^{-1} -1240 cm^{-1} is attributed to the vibration of the B-O^- terminal groups in pyroborate units [24,28,31-32]. The band towards1270 cm^{-1} is attributed to the asymmetric elongation mode B-O in orthoborate units (BO_3).

Table 3. Frequencies I.R assignments of (0.95-x) Bi_2O_3-x B_2O_3-0.05[P_2O_5-Nb_2O_5]

Sample	BA_6	BA_7	BA_8	BA_9	BA_{10}
x	0.30	0.35	0.4	0.45	0.5
squelettes Bi-O-Bi	413	434	410	403	426
ou squelettes B-O-Bi		468	446	457	454
ou squelettes B-O-B		484	482	510	496
métaborates $\upsilon_{a\ B\text{-}O\text{-}Nb}$	636	657	669	672	675
métaborates $\upsilon_{a\ B\text{-}O\text{-}P}$	692	692	693	693	695
orthophosphates	695	721	-	-	-
boroxol	905	860	885	-	
orthoborates BO_3	997	965	961	953	904
BO (BO^{4-})	1025	1034	1026	1030	1048
pyroborates B-O^-	1221	1227	1230	1238	1241
υ_{as}(BO) dans BO_3	1316	1383	1383	1383	1384

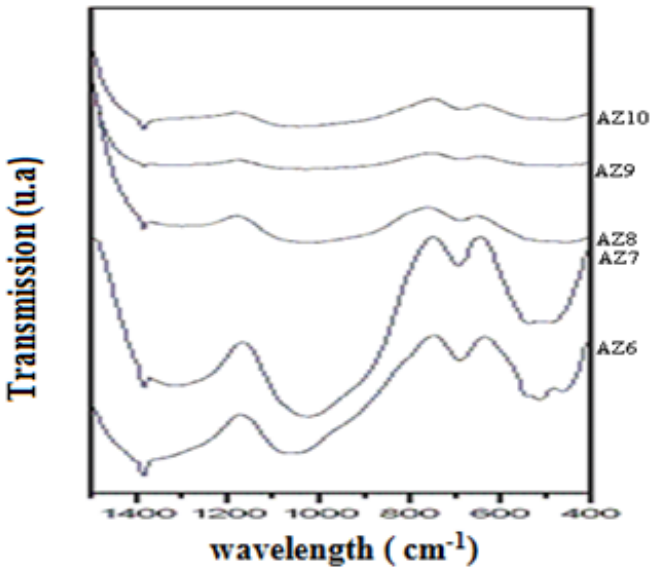

Fig. 4. IR spectrums of (0.90-x) Bi_2O_3-x B_2O_3-0.1 [P_2O_5-Nb_2O_5]

Table 4. Frequencies I.R assignments of (0.90-x) Bi_2O_3-x B_2O_3-0.1 [P_2O_5-Nb_2O_5]

	AZ_6	AZ_7	AZ_8	AZ_9	AZ_{10}
x	0.30	0.35	0.4	0.45	0.5
squelette Bi-O-Bi	478	468	459	460	460
ou squelettes B-O-Bi	-	515	497	484	508
ou squelettes B-O-B	537	533	542	500	536
métaborates $\upsilon_{a\ B\text{-}O\text{-}Nb}$	654	670	670	671	-
métaborates $\upsilon_{a\ B\text{-}O\text{-}P}$	692	692	693	691	687
Boroxol	884	896	891	894	
BO (BO^{4-})	1025	1034	1068	1027	1037
Pyroborates B-O^-	1291	1290	1264	-	-
υ_{as}(BO) dans BO_3	1383	1383	1383	1383	1384

Otherwise, the increase of Nb_2O_5 and P_2O_5 concentrations results in:
- Decrease in the intensity of the band corresponding to the B-O-P groups.
- Disappearance of the Bi-O-B bands and those assigned to the orthoborate and orthophosphate groups.
- Displacement of the band corresponding to the pyroborates BO^- to the high frequencies.

3.4. Corrosion inhibition

3.4.1. Optimal formulation of additives

Initial SIE investigations have been carried out to determine the optimal formulation of the additives to improve the corrosion resistance of the carbon steel. The Nyquist impedance diagrams obtained for (AZ) do not have perfect semicircles due to the frequency dispersion (Fig. 5). The electrochemical parameters derived from these diagrams and the values of the inhibition efficiencies are given in Table 5. We see that the charge transfer (R_{ct}) increase in with additives. The maximum value is reached for AZ6. Thus, the electrochemical study was carried out on the AZ6 and BA6 formulation.

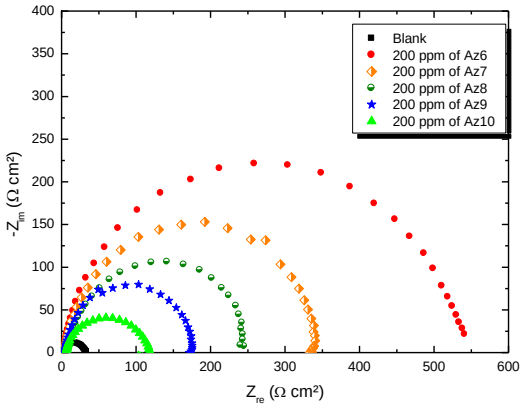

Fig. 5. EIS spectra at the corrosion potential of steel in HCl 1 M without and with 200 ppm of series AZ

Table 5. Electrochemical parameters from the EIS spectra and the values of the inhibition efficiency of carbon steel in 1.0 M HCl without and with 200 ppm of AZ series

	R_{ct}(ohm.cm²)	Q_{dl}(µf/cm²)	E%	Θ
Blank	35	284	-	-
AZ6	550	120	93.6	0.93
AZ 7	340	163	89	0.89
AZ8	248	183	86	0.86
AZ 9	179	201	80	0.80
AZ 10	120	251	71	0.71

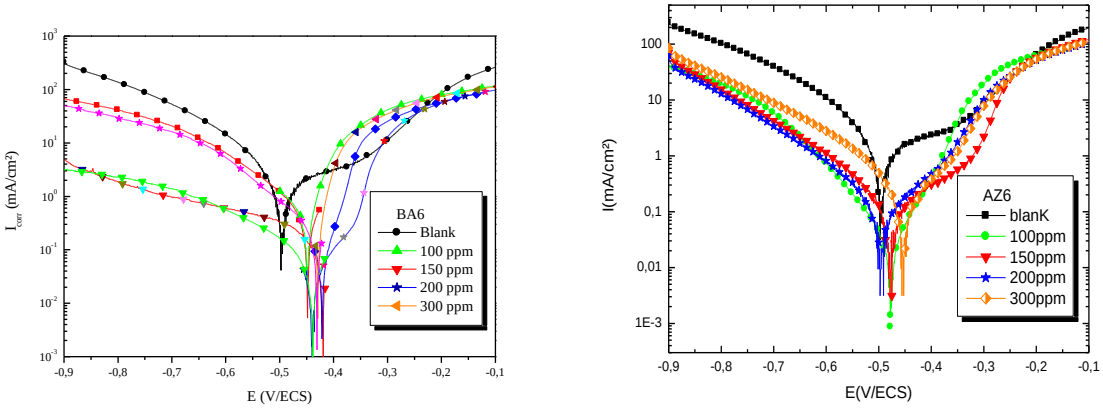

Fig. 6. Polarization curves of steel in HCl 1 M with additives at different concentration

3.4.2. Concentration effect

Our approach consists in optimizing the concentration of the two compounds AZ6 and BA6 in order to obtain the best inhibitory efficiency.

Table 6. Electrochemical parameters of carbon steel at different concentrations of BA6 in 1.0 M HCl.

C (M) de BA6	Ecorr (mV/Ag/AgCl)	–βc (mV/dec)	Icorr (µA cm^{-2})	E (%)	Θ
Témoin	-497	92	983	-	-
100ppm	-429	111	320	67	0.67
150ppm	-406	203	231	76.5	0.765
200ppm	-447	108	44	95.5	0.955
300ppm	-439	115	112	88.6	0.886

Table 7. Electrochemical parameters of carbon steel at different concentrations of AZ6 in 1.0 M HCl

Cinh(M) de AZ6	Ecorr	Bc (mV dec-1)	I_{corr} (µA/cm^2)	E%	Θ
Témoin	-497	-92	983	-	-
100ppm	-478	-95	361	63	0.63
150ppm	-479	-102	204	79	0.79
200ppm	-498	-80	70	93	0.93
300ppm	-454	-110	121	87.6	0.876

Figure 6 present the polarization curves of the carbon steel in 1M HCl with and without the compounds AZ6 and BA6. The addition of AZ6 at different concentrations from 100 ppm to 300 ppm to the corrosive solution led to a displacement of the corrosion potential E_{corr} to the anodic values, in contrast to the BA6 addition, where the corrosion potential is virtually unchanged.

Moreover, we observe a decrease of the cathodic current in the presence of the two glasses, the variation of the current in the anodic side is less pronounced. It would appear that these two compounds strongly inhibit the evolution of hydrogen and slightly anodic reaction. Thus, we recorded a decrease in the corrosion current with a maximum efficiency at a concentration of 200 ppm in AZ6 and BA6 (Tables 6 and 7).

These results indicate that BA6 and AZ6 glasses act as mixed type inhibitors with a predominant cathodic efficiency. The values of the cathode slope (bc) remain practically constant indicating that these molecules do not affect the hydrogen evolution mechanism [6].

3.5. Electrochemical impedance spectroscopy (EIS)

The corrosion inhibition of the carbon steel in acidic medium (1M HCl), in the presence of BA6 and AZ6, was analyzed by Electrochemical impedance spectroscopy (EIS). The figure 7 present the impedance spectra traced at the corrosion potential E_{corr} after 0.5 h of immersion. from these spectra we remark a single capacitive loop, attributed to the transfer of charge process, whose diameter increases with the concentration of compounds BA6 and AZ6 [33].The figure 8 show the equivalent circuit model employed to extract the electrochemical parameters .

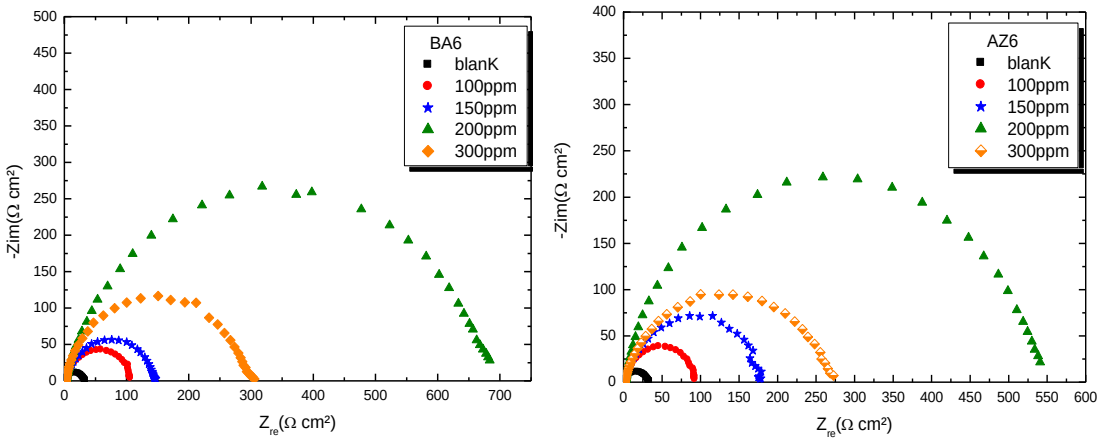

Fig. 7. Impedance diagrams of the steel electrode at E_{corr} after 0.5 h of immersion in acidic medium with and without AZ6

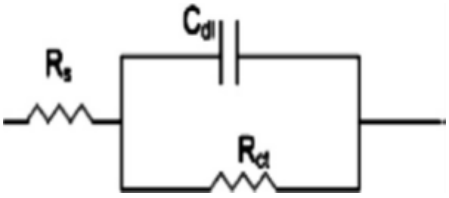

Fig. 8. The equivalent circuit model used to fit the Impedance diagrams

The higher value of charge transfer and inhibition efficiency are obtained at a concentration of 200 ppm for both glasses AZ6 and BA6 confirming their inhibitory effect (Table 8 and 9).

Table 8. Electrochemical parameters extracted from EIS data of carbon steel at different concentrations of BA6 in 1M HCl

Cinh (M) of BA6	Rct(ohm.cm²)	C_{dl}(µf/cm²)	E%	Θ
témoin	35	284	-	
100ppm	104	240	66	0.66
150ppm	149	224	76.5	0.765
200ppm	700	88	95	0.95
300ppm	305	111	88.5	0.886

Table 9. Parameters extracted from EIS data of carbon steel at different concentrations of AZ6 in 1M HCl

Cinh (M) of AZ6	Rct(ohm.cm²)	C_{dl}(µf/cm²)	E%	Θ
Témoin	35	284	-	
100ppm	94	240	62.7	**0.627**
150ppm	175	191	80	**0.80**
200ppm	550	120	93.6	**0.936**
300ppm	274	144	87	**0.87**

The variation of C_{dl} may be result from a decrease in the local dielectric constant and / or an increase in its thickness [34]. This would indicate that the BA6 and AZ6 molecules would adsorb to the steel/1 M HCl interface by replacing the water molecules, thus inhibiting the dissolution reaction [6,35].

3.6. Effect of temperature

The thermodynamic study can provide the information on interactions type between inhibitor and steel. These interactions are related to the nature of the electrode used, the chemical structure of the inhibitor and the electrolyte. Two main types of interaction can describe the adsorption of the compounds: physical adsorption or chemisorption.

The polarization curves, with and without 200 ppm of BA6 and 200 ppm of AZ6, at different temperatures, are shown in figures 9 and 10. We note that the values of corrosion current i_{corr} increase with temperature as reported by several authors. The corresponding electrochemical parameters are shown in tables 10, 11 and 12.

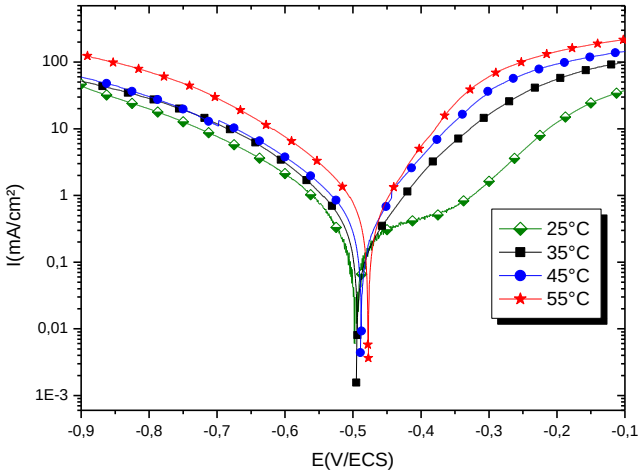

Fig. 9. Polarization curves of carbon steel in acidic medium 1.0 M HCl at different temperature

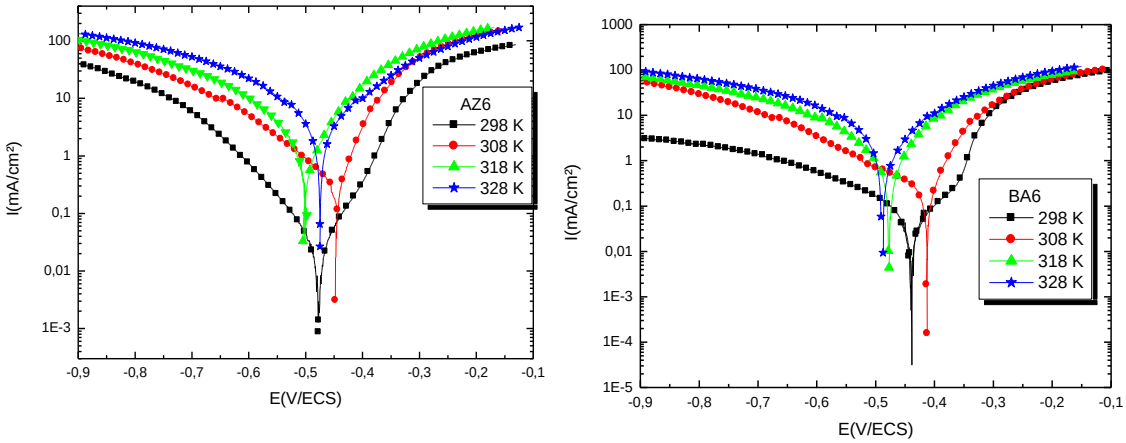

Fig. 10. Polarization curves of carbon steel in blank solution 1.0 M HCl with 200 ppm of AZ6 and BA6 at different temperature

Table 10. Electrochemical parameters extracted from polarization curve of carbon steel at different temperatures in 1.0 M HCl solution

	E_{corr}(mV/ag/agcl)	I_{corr}(mA/cm²)	β_c mV
25C°	-498	0.983	-92
35 C°	-491	1.6	-178
45 C°	-475	2.42	-165
55 C°	-465	3.1	-151

Table 11. Electrochemical parameters of steel at different temperatures in HCl 1M with BA6

BA6	Ecorr(mV/ECS)	Icorr(µA/cm²)	Bc mV
298	-447	44	-108
308	-410	162	-171
318	-476	302	-45
328	-489	598	-113

Table 12. Electrochemical parameters of steel at different temperatures in HCl 1M with BA6

AZ6	Ecorr(mV/ECS)	Icorr(mA/cm²)	Bc mV
298	-498	70	-80
308	-444	178	-86
318	-512	342	-98
328	-491	620	-110

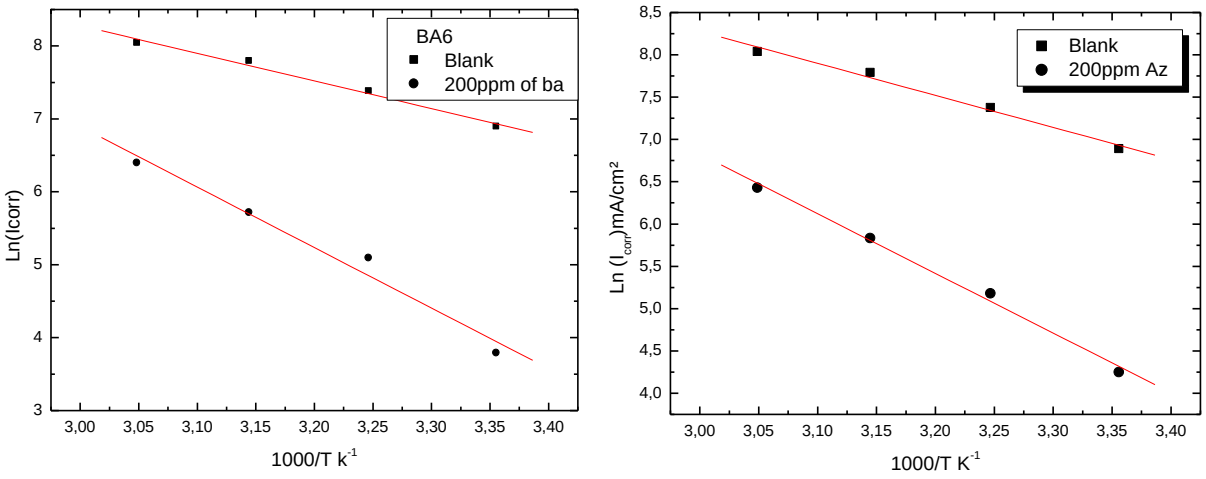

Fig. 11. Ln (i_{corr}) as a function of (1/T) in 1.0 M HCl medium in the absence and the presence of and without 200 ppm

The plots of Ln (i_{corr}) as a function of the 1/T are presented in Figure 11. We can observe that a linear variation with correlation coefficients (c.c) close to 1. Thus, the energy activation E_a for the corrosion process of carbon steel was calculated from the Arrhenius model by following the equation (6):

$$\text{Ln } i_{corr} = \text{Ln A} - \frac{Ea}{RT} \qquad (6)$$

-R_{ct}: Transfer resistance
-E_a: activation energy,
- A: Pre-exponential factor,
R: Universal gas constant
-T: Absolute temperature.

To better understand the corrosion inhibition process, it would also be interesting to determine the enthalpy and the entropy of activation. These parameters were extracted from the Arrhenius equation (7):

$$\mathrm{Ln}\frac{icorr}{T} = (\ln(\frac{R}{Nh}) + \frac{\Delta Sa}{R}) - \frac{\Delta Ha}{RT} \quad (7)$$

Where h: Planck constant, N: Number of Avogadro, R: Universal gas constant, ΔH_a: Enthalpy of activation, ΔS_a: Entropy of activation.

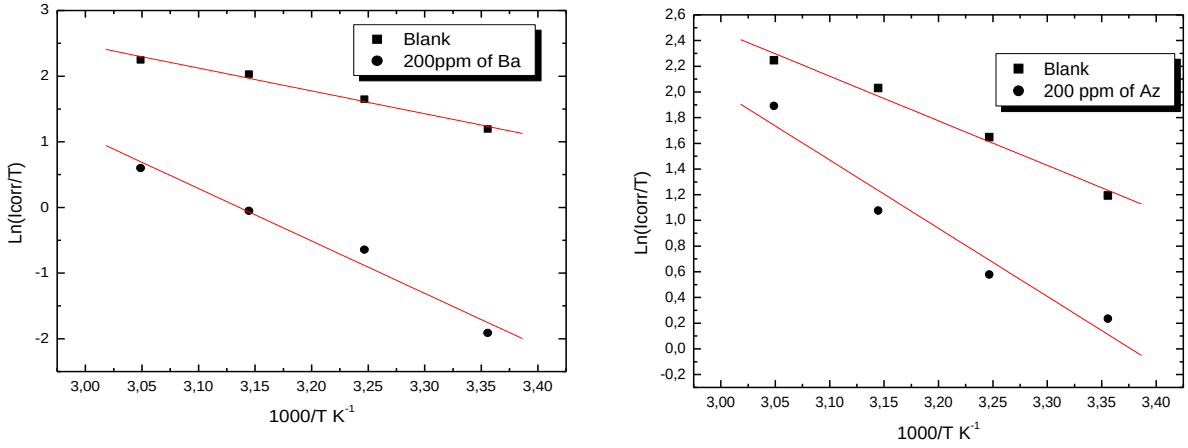

Fig. 12. Ln (i_{corr}/T) as a function of (1/T) in 1 M HCl with and without 200 ppm (a) BA6; (b) AZ6

Indeed, the plot of Ln (i_{corr}/T) as a function of 1000 / T (Figure 12) gives straight lines whose slopes have made it possible to determine ΔH^*_a and the intersection with the ordinates axis, ΔS^*_a for BA6 and AZ6 (Table 13). From this table we can observe that the ΔH_a is lower than E_a which means that the molecule of these inhibitors form a stable layer on the steel surface [36].

Table 13. The value of thermodynamic parameters E_a, ΔH^*_a , ΔS^*_a for carbon steel in 1.0 M HCl with and without 200 ppm of additives

	E_a KJ/mol	**ΔH_a^* KJ/mol**	**ΔS_a^* KJ/mol**
HCl 1M	31.5	28	-107
HCl +200 ppm BA6	69	66.3	-122
HCl + 200ppm AZ6	58.6	44	-63.2

The large negative values of entropies ΔSa* imply that the activated complex in the rate determining step represents an association rather than a dissociation step, meaning that a decrease in disordering takes place on going from reactants to the activated complex [37].The activation energies E_a being higher for the solutions containing the compounds BA6 and AZ6 would assume that the adsorption is a physical type.

3.7. Adsorption isotherm

The adsorption isotherm give information on the interaction between the metal and inhibitor. Surface coverage was calculated by following equation (8):

$$\frac{C}{\theta} = \frac{1}{K} + C \qquad (8)$$

The θ values for different inhibitor concentrations are tested by applying various isotherms (Frumkin, Temkin and Langmuir). The best one was the Langmuir isotherm. According to this isotherm, θ is related to concentration inhibitor C via equation (8) and (9):

$$LogK = -1.74 - \left(-\frac{\Delta G^0_{ads}}{2.303RT}\right) \qquad (9)$$

where

-K was the adsorptive equilibrium constant

- $\Delta G°_{ads}$ was the free energy of adsorption [38].

Indeed, the Figure 13 shows that the plots of C/ɵ as a function of concentration correspond to a straight line with a slope close to 1, this indicate that the adsorption of the two compounds on the carbon steel in the acidic solution obeys the Langmiur model.

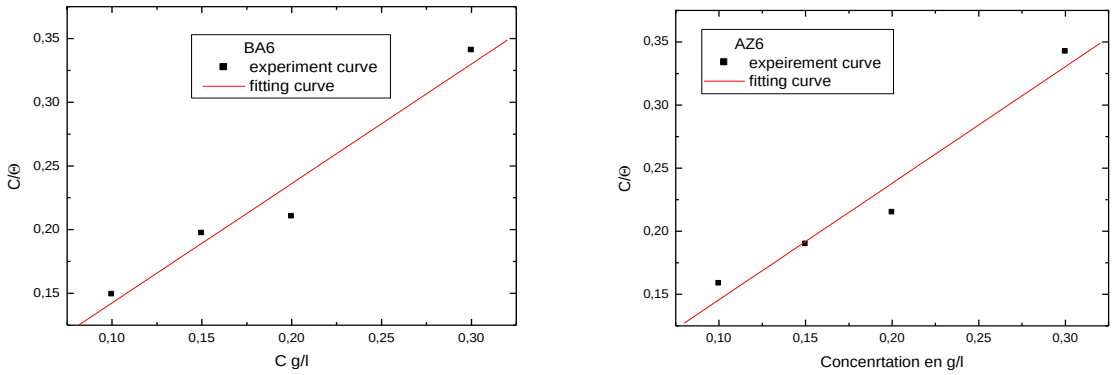

Fig. 13. Langmuir adsorption isotherm plot for carbon steel in 1 M HCl at different concentrations of AZ6 and BA6 at 298 K

The free energy ΔG^0_{ads} value of the adsorption calculated by the above formula is equal to -17.43 kj/mol for BA6 and equal to -17.2 for AZ 6. This negative value indicate that the adsorption of BA6 and AZ6 on the surface of steel was a spontaneous process [39]. When the the values of ΔG^0_{ads} higher than -20 kJ/mol indicate a physisorption and if the value lower than is associated with chemisorption [40-45]. The ΔG^0_{ads} value of BA6 and AZ6 being slightly greater than -20 kJ/mol confirms that the adsorption process of BA6 and AZ6 is the physisorption nature.

4. CONCLUSION

The glasses of the Bi_2O_3-B_2O_3-[$0.5P_2O_5$-$0.5Nb_2O_5$] system were prepared and then characterized by X-ray diffraction, this allowed the delimitation of the vitreous zone. The Fourier Transform Infrared spectroscopy study showed that pyroborate units appear for high boron content in the vitreous domain. The increase of the Nb_2O_5 and P_2O_5 contents leads to a decrease in the B-O-P and Bi-O-B groups with a gradual disappearance of the orthoborate groups and displacement of the band corresponding to the BO^- pyroborates to the high frequencies.

The corrosion inhibition of the carbon steel corrosion in 1.0 M HCl solution by the glasses of the Bi_2O_3-B_2O_3-[$0.5P_2O_5$-$0.5Nb_2O_5$] system was examined by different electrochemical methods. The results showed a significant decrease in the corrosion current and an important increase in transfer resistance when the vitreous compounds were added to the corrosive solution. This inhibition depends on the composition of the vitreous phase. The inhibitory efficiency reaches 95% at a concentration of 200 ppm for the two additives. The system acts primarily as an anodic inhibitor by formation a stable film on electrode surface.

The thermodynamic study showed that this film was formed by physisorption. The adsorption mechanism obeys to the Langmuir adsorption model.

REFERENCES

[1] R. Salghi, L. Bazzi, B. Hammouti, and S. Kertit, Bull. Electrochem. 16 (2000) 272.
[2] L. Larabi, Y. Harek, O. Benali, and S. Ghalem, Prog.Org. Coat. 54 (2005) 256.
[3] M. Mihit, K. Laarej, H. Abou E. Makarim, L. Bazzi, R. Salghi, and B. Hammouti, Arab. J. Chem. 3 (2010) 55.
[4] O. Benali, L. Larabi, S. Merah, and Y. Harek, J. Mater. Environ. Sci. 2 (2011) 39.
[5] M. Galai, M. Rbaa, Y. El Kacimi, M.Ouakki, N. Dkhirech, R. Touir, E. Lakhrissi, and M. Touhami, Anal. Bioanal. Electrochem.9 (2017) 80.
[6] O. Benali, L. Larabi, S. M. Mekelleche, and Y.Harek, J. Mater. Sci. 41 (2006)7064.
[7] S.Merah, L.Larabi, O.Benali, and Y.Harek, Pig. Res. Tech. 37 (2008) 291.
[8] D. Ben Hmamou, R. Salghi, A. Zarrouk, H. Zarrok, B. Hammouti, S. S. Al-Deyab, M. Bouachrine, A. Chakir, and M.Zougagh, Int. J. Electrochem. Sci. 7 (2012) 5716.
[9] W. D. Robertson, J. Electrochem. Soc. 98 (1951) 94.
[10] G. H. Cartledge, Corrosion 24 (1968) 223.
[11] C. Breslin, G. Treacy, and W. Carroll, Corros. Sci. 36(1994) 1143.
[12] W. Badawy, F. Al-Kharafi, and A. El-Azab, Corros. Sci. 41 (1999) 709.
[13] A. Kolics, A. Besing, and A. Wieckowski, J. Electrochem. Soc. 148 (2001) B321.
[14] T.Wu, W.Tsai, Corros. Sci. 45 (2003)267.
[15] M. R.Ali, C. M. Mustafa, and M. Habib, J. Sci. Res. 1 (2009) 82.
[16] R.R. Podor, N. David, C. Rapin, M. Vilasi, and P. Berthod, Corros. Sci. 49 (2007) 3226.
[17] T. Guedira, Contributionà l'identification des isothermes vers 820 °C des ternaires MO_X -Bi_2O_3- P_2O_5 (M=Li, Ca, Ba, B, Sb, Zr, Sn, Nb, Ta). Etude des phases, sillenite, fluorine et vitreuses. Thèse de Doctorat D'Etat ES-Sciences. Université Ibn Tofail, Faculté des sciences, Kenitra (2003).
[18] M. Belfaquir, T. Guedira, S. D. Elyoubi, and J.L. Rehspringe. Ann. Chim. Sci. Matériaux 30(2005) 27.
[19] M. Belfaquir, T. Guedira, S. D. Elyoubi, and J.L. Rehspringer,Sci. Lib Editions Mersenne 5 (2013) N°130302.
[20] J. Zarzycki, les verres et l'état vitreux, ed. Masson, Paris (1982).
[21] W.H. Zachariasen, J. Am. Chem. Soc. 54 (1932) 3841.
[22] K. H. Sun, J. Am. Soc. 30 (1947) 277.
[23] V.M. Goldschmidt, and I. Mat, NaturwissKlasse7 (1926) 156.
[24] U.H. Zachariasen, J.Am. chem. Soc. 54 (1932) 381.
[25] Y. Dimitrivo, J. Nom. Cryst. Sol. 95-96 (1987) 937.
[26] A. J. Semkal, J. Soc. Glass.Technol. 35 (1951) 411T.
[27] J.E. Stanworth, J. Soc. Glass. Technol. 30, (1946) 54T ; 32 (1984) 154T, 366T ; 36 (1952) 217T.
[28] L. Pauling, The nature of the chemical bond. 3ed.cornell Ithaca (1960).

[29] M. R. Ali, C. M. Mustafa, and M. Habib, J. Sci. Res. 1 (2009) 82.
[30] E. Kordes, and E.Worster, Glass bar 32 (1957) 276.
[31] T. Takahashi, H. Iwahara, and Y.Nagai, J. AppelElectroch. 2 (1972) 97.
[32] G. Gattow, and D.Chutze, Zeit Anorg. Allg. Chem. 328 (1964) 44.
[33] O. Benali, L. Larabi, M. Traisnel, L. Gengenbre, and Y. Harek, Appl. Surf. Sci. 253 (2007) 6130.
[34] H. F.Finley, and N. Hackerman, J. Electrochem. Soc. 107 (1960) 259.
[35] N. Hackerman, E. S. Snavely, and J. Payne, J. Electrochem. Soc. 113 (1966) 677.
[36] W. Li, Q. He, C. Pei, and B. Hou, Electrochim. Acta 52 (2007) 6386.
[37] L. Afia, R. Salghi, A. Zarrouk, H. Zarrok, O. Benali, B. Hammouti, S. S.Al-Deyab, A. Chakir, and L. Bazzi, Electrochim. Acta 30 (2012) 267.
[38] Y. Abboud, A. Abourriche, T. Saffaj, M. Berrada, M. Charrouf, A. Bennamara, N. AlHimidi, and H. Hannache, Mater. Chem. Phys. 105 (2007) 1
[39] J.O'M, Bockris,and D. A. Swinkels, J. Electrochem. Soc. 111 (1964) 736.
[40] J.O'M, Bockris, and D. Drazic, Electrochim. Acta 7 (1962) 293.
[41] V. Branzoi, F. Branzoi, and M. Baibarac, Mater. Chem. Phys. 65 (2000) 288.
[42] M. Cissé, M. Abouchane, T. Anik, K. Himm, R. A. Belakhmima, M. EbnTouhami, R. Touir, and A. Amiar, Int. J. Corros. (2010).
[43] A. Fattah-Alhosseini, and M. Noori, Anal. Bioanal. Electrochem. 8 (2016) 145.
[44] A. Fattah-Alhosseini, and B. Hamrahi, Anal. Bioanal. Electrochem. 8 (2016) 535.
[45] A. Elbadaoui, M. Galai, M. Cherkaoui, and T. Guedira, Der Pharma Chem. 8 (2016) 214.